

SURFACE WAVE SPECTRA

by

P.A. Crowther
Naval Division
Marconi Space and Defence Systems Ltd
Frimley, Surrey, England, U.K.
U.S.A.

ABSTRACT

A classification is made of the different types of wave elevation spectra namely 1D time spectra, 1D spatial spectra, 2D spatial spectra and 3D space-time spectra. Relations with simple single parameter measures of surface wave slope and significant wave height are also stated. Wave measurement devices are examined, including wave staffs, spar buoys, combined motion and wave-probe devices, Laser and Radar altimeters, the inverted echo sounder, radar scatterometers, stereophotography and Fourier transform photography. Theoretical mechanisms for wave generation are reviewed critically. The state of progress in understanding of the equilibrium spectrum, the re-distribution of wave energy, swell waves and overshoot effect, is examined. Finally an attempt is made to summarize experimental knowledge, and show where from an acoustics viewpoint it is incomplete, where from a wave dynamics viewpoint current theory is inadequate and where both might be improved.

1. INTRODUCTION

Sea surface waves are significant to underwater acoustics because they scatter sound and produce Doppler broadening and frequency shift on scattered and reflected sound. Backscattering at small grazing incidence tends to be primarily a first order Bragg effect, the dominant wavelength in the sea surface being of order half the acoustic wavelength, modified by the surface slope produced by the longer waves. Thus if we consider sonar frequencies from say ~ 0.1 to ~ 100 kHz, the primary backscatter wavelength component in the surface is from ~ 1 cm. to ~ 10 m. For the slope modulation and Doppler effects, one should also include longer wavelengths, up to the wavelength beyond which negligible slope is carried. This is usually at length $\lesssim 500$ m. At high frequencies the last 2 octaves up to 100 kHz are of somewhat rarer application, and the effect of bubbles will tend to dominate at such frequencies anyhow, so that we could expect that for backscatter, the strongest interest is over a surface wavelength band of ~ 5 cm to 10m., with some interest between 500m to 10m and 5cm to 1cm. For forward propagation, the prime interest is at longer wavelengths, where the slope spectrum is highest, say from 500m to 1m.

To convert these wavelengths into wave frequency, we need to use the dispersion laws for surface waves, which are

$$n^2 = gk + \gamma k^3 \quad (1)$$

$$c = n/k = (g/k + \gamma k)^{\frac{1}{2}}, \quad (2)$$

$$v_0 = dn/dk = \frac{1}{2} (g + 3 \gamma k^2) / n, \quad (3)$$

where g = gravity

$$n = 2\pi f = 2\pi \text{ times surface frequency (radian sec}^{-1}\text{)}$$

$$k = 2\pi/\Lambda = 2\pi/\text{surface wavelength}$$

$$\gamma = \text{surface tension/water density} = 7.4 \cdot 10^{-5} \text{ m}^3 \text{ s}^{-2}$$

$$c = \text{surface phase speed}$$

$$v = \text{surface group speed}$$

Taking these laws for present at face value, the surface frequency bands of strongest interest we find become $\sim 0.5\text{Hz}$ to 10Hz for backscatter, and $\sim 0.05\text{Hz}$ to $\sim 1\text{ Hz}$ for propagation, with an overall band of say 0.05Hz to $\sim 50\text{Hz}$.

These waves have phase speeds, c , from 0.23 to 30 m/s and v from 0.18 to 15 m/s . Caveats on taking (1-3) at face value are given in Sections 8 and 9.

Waves for which the first term on the right in (1) dominates are called gravity waves; those for which the second dominates are called capillary waves. It is convenient to define the transition, conventionally where the gravity and surface tension forces are equal, that is at

$$k = k^* = (g/\gamma)^{\frac{1}{2}} = 364 \text{ rad/m}$$

$$\Lambda = \Lambda^* = 2\pi/k^* = 1.7 \text{ cm}$$

$$n = n^* = (4g^3/\gamma)^{\frac{1}{4}} = 85 \text{ rad sec}^{-1}$$

$$f = f^* = n^*/2\pi = 13.5\text{Hz}$$

$$c = c^* = (4g\gamma)^{\frac{1}{4}} = 0.23 \text{ ms}^{-1}$$

$$v = v^* = 0.23 \text{ ms}^{-1}$$

Clearly sonar interest only just extends into the capillary regime at the very highest frequencies. For the majority of applications, we are interested only in gravity waves, albeit often rather short ones for which:

$$n^2 = gk \quad (4)$$

$$c = g/n = (g/k)^{\frac{1}{2}}, \quad (5)$$

$$v = \frac{1}{2}c \quad (6)$$

2. DEFINITION OF WAVE SPECTRA

Spectra are measured of either the wave elevation or slope as a function of temporal or spatial radian frequency n or k respectively, and in 1, 2, or 3 dimensions. Nomenclature and normalization vary enormously and are frequently confusing in the literature. For the present purpose, we use a unified kernel index approach, the kernel indicating the variable, elevation or slope, analysed, and the index denoting the number of dimensions.

Power Spectra are most conveniently defined from the space time covariance function:

$$Z(\underline{r}, t) = \langle z(\underline{r}' + \underline{r}, t' + t) z(\underline{r}', t') \rangle \quad (7)$$

for spatio-temporal lag \underline{r}, t in 2 spatial and 1 temporal dimensions, z denoting the surface elevation with respect to mean level. The most general power spectrum is then the spatio-temporal

$$E_3(\underline{k}, n) = (2\pi)^{-3} \int \int \int_{-\infty}^{\infty} Z(\underline{r}, t) \exp(-i\underline{k} \cdot \underline{r} - int) d^2r dt, \\ (-\infty < k_1, k_2, n < \infty, E_3(\underline{k}, n) \equiv E_e(-\underline{k}, -n)) \quad (8)$$

Fine though this is in theory, it is too complicated to have been measured in practice, so that we must define less ambitious spectra. We may define an unoriented spatial spectrum

$$E_2(\underline{k}) = \int_{-\infty}^{\infty} E_3(\underline{k}, n) dn = \int \int_{-\infty}^{\infty} Z(\underline{r}, c) \exp(-i\underline{k} \cdot \underline{r}) d^2r \quad (9)$$

$$(-\infty < k_1, k_2 < \infty), E_2(\underline{k}) \equiv E_2(-\underline{k})$$

This is the spectrum required in acoustic scattering theory for all aspects other than Doppler effect, and is the spectrum measured by radar scatter, but it is not usually quoted in this form by wave spectroscopists, who tend to use an oriented two dimensional spectrum, the exact definition of which is not specified, but where vector \underline{k} is associated not just with the time frozen surface, but with the direction of propagation.

A reasonable mathematical definition might be:-

$$E_{2D}(\underline{k}) = 2 \int_{-\infty}^0 E_3(\underline{k}, n) dn \quad (10)$$

$$(-\infty < k_1, k_2 < \infty, E_{2D}(\underline{k}) + E_{2D}(-\underline{k}) = 2 E_2(\underline{k}), E(\underline{k}) \neq E(-\underline{k}))$$

For a wave system strictly obeying the dispersion laws, of course, no problem in definition arises, because $E_3(\underline{k}, n)$ vanishes at all points in n other than $\pm (gk + \gamma k^3)^{\frac{1}{2}}$, where E_3 has a δ -function. In practice non linear effects broaden this out. E_2 and E_{2D} will also be referred to by cartesian or polar components when required, e.g.

$$E_{2D}(\underline{k}) d^2k \equiv E_{2D}(k_1, k_2) dk_1 dk_2 \equiv E_{2D}(k, \theta) k dk d\theta \quad (11)$$

The 2 dimensional spectra may be condensed into a 1 dimensional omnidirectional spatial spectrum =

$$E_1(k) = k \int_0^{2\pi} E_2(k, \theta) d\theta = k \int_0^{2\pi} E_{2D}(k, \theta) d\theta \quad (12)$$

$$(0 < k < \infty)$$

The temporal power spectrum may be defined by:-

$$E(n) = \pi^{-1} \int_{-\infty}^{\infty} Z(o, t) \exp(-int) dt$$

$$(0 < n < \infty) \quad (13)$$

For a wave system obeying the dispersion relations, we have $E(n) dn = E(k) dk$, so that:-

$$E(n) = 2n\{g + 3\gamma k(n)^2\}^{-1} E_1\{k(n)\} \quad (14)$$

$E(n)$ is the commonest wave spectrum directly measured, since it is a point spectrum, so that more frequently we are interested in reversing the transformation in (14). Another commonly measured spectrum is the planar elevation spectrum - the power spectrum of z as a 1 dimensional profile through a vertical plane.

$$E_{1D}(k_1) = \int_{-\infty}^{\infty} E_{2D}(k_1, k_2) dk_2 \quad (15)$$

$$(-\infty < k_1 < \infty)$$

where the coordinate system $\underline{k} = k_1, k_2$ is chosen so that $\underline{k} = (k_1, 0)$ is in the plane concerned. An unoriented planar spectrum may be defined by $E_{1U}(k_1) = (E_{1D}(k_1) + E_{1D}(-k_1))$ ($0 < k_1 < \infty$) (16)

Surface slope may also be described by power spectra, the commonest forms being

(a) Cartesian Component slope

$$S_{2,i,j}(\underline{k}) \equiv k_i k_j E_2(\underline{k}), \quad (i = 1, 2; j = 1, 2) \quad (17)$$

$$S_{2D,i,j}(\underline{k}) \equiv k_i k_j E_{2D}(\underline{k}) \quad (18)$$

$$S_{ij}(n) = \pi^{-1} \int_{-\infty}^{\infty} \langle z_i(o, t' + t) z_j(o, t') \rangle \exp(-int) dt \quad (19)$$

where subscripts on $z(\underline{r}, t)$ denote cartesian gradient components

(b) Total slope spectra, such as

$$S_1(k) = k \int_0^{2\pi} (S_{2,1,1}(k, \theta) + S_{2,2,2}(k, \theta)) d\theta, \quad (20)$$

$$= k^2 E_1(k)$$

$$S(n) = S_{11}(n) + S_{22}(n) \quad (21)$$

$$\text{For dispersion law obedient spectra } S(n) = k^2(n) \cdot E(n) \quad (22)$$

The above definitions are made so that the normalization of spectra is as simple as possible, that is

$$\begin{aligned} \sigma^2 &= \int_{-\infty}^{\infty} \int_{-\infty}^{\infty} \int_{-\infty}^{\infty} E_3(\underline{k}, n) d^2k dn = \int_{-\infty}^{\infty} \int_{-\infty}^{\infty} E_2(\underline{k}) d^2k \\ &= \int_{-\infty}^{\infty} \int_{-\infty}^{\infty} E_{2D}(\underline{k}) d^2k = \int_0^{\infty} E_1(k) dk = \int_0^{\infty} E(n) dn \\ &= \int_{-\infty}^{\infty} E_{1D}(k_1) dk_1 \end{aligned} \quad (23)$$

σ^2 being height variance, and

$$\sigma_{ij}^2 = \iint_{-\infty}^{\infty} S_{2, i, j}(\underline{k}) d^2k = \iint_{-\infty}^{\infty} S_{2D, i, j}(\underline{k}) d^2k = \int_0^{\infty} S_{ij}(n) dn, \quad (24)$$

$$\sigma_{ij}^2 \text{ being covariance of slopes } z_i(\underline{r}, t) \text{ and } z_j(\underline{r}, t), \text{ also}$$

$$\sigma_s^2 = \int_0^{\infty} S_1(k) dk = \int_0^{\infty} S(n) dn, \quad (25)$$

where $\sigma_s^2 = \sigma_{11}^2 + \sigma_{22}^2 = \text{total slope variance.}$

3. SPECIFICATION OF GENERATING CONDITIONS

The wind over the sea has been found to be fairly well represented by the logarithmic profile characteristic of turbulent flow

$$U(z) = (U_*/K) \ln(z/z_0) \quad (26)$$

U being windspeed at height z , $K = 0.41 = \text{Von Kármán's constant,}$

U_* the friction speed defined by

$$U_*^2 = T/\rho = C_D U(z)^2 \quad (27)$$

where $T = \text{drag stress, } \rho = \text{air density, } C_D \text{ the drag coefficient at height } z,$
and z_0 a roughness constant depending on windspeed.

Numerous measurements of C_D have been made, and different empirical formulae proposed. Thus Phillips (1966) shews collected experimental values of C_D at 10 metres of $C_{10} \approx 0.5 \cdot 10^{-3}$ to $2 \cdot 10^{-3}$ depending partially on windspeed, Deacon and Webb (1962) quote $C_{10} \approx 10^{-3} + 7 \cdot 10^{-5} U_{10}$ (MKS), Sheppard (1958) quotes $C_{10} = (0.8 + 0.1U) 10^{-3}$, (MKS). Cardone (1969) quotes:-

$$C_D \approx K/\ln \{z/(0.684U_*^{-1} + 4.28 \cdot 10^{-5} U_*^2 - 0.443)\}, (\text{cgs}),$$

using which values Pierson and Stacy (1973) have computed U_{10} and $U_{19.5}$ versus U_* . For windspeeds from 1-15 m/sec., C_D ranges from about 10^{-3} to $2 \cdot 10^{-3}$, and U/U_* from about 20 to 30. A reasonable average ratio for approximate conversion would be:

$$U/U_* \sim 27 \quad (U = 1-15 \text{ m/sec.})$$

U being measured at any reasonable anemometric height, e.g. 7.5, 10, 19.5m. The differences between velocity at different practical heights are less than those due to uncertainty in C_D . Further references to C_D can be found in Hasselmann et al (1973).

Fetch is defined as the distance over which the wind has been blowing, and may be denoted as X. Similarly duration of wind may be denoted by T. For a given wave component, equivalent fetch and duration may be related by comparing T with $X/v=2X n/g$. If the former is greater, conditions are fetch limited, whilst otherwise they are duration limited.

Because to a large extent the mechanics of sea waves is a scale free process, in that gravity waves of one size are scale models of one another, and the logarithmic profile is essentially scale free away from the surface, there should be a principle of dimensional similarity governing wave spectral shape and growth, as shewn by Kitaigorodskii (1962). We can expect any spectrum in principle to be a function of only a five variables, thus e.g.

$$E(n) = \phi(n, X, g, U_*, T) \quad (28)$$

Dimensional similarity then insists that the functional form of ϕ should be universal if dimensionless forms are used to remove g and U_* as scaling constants. We therefore use the following

$$\begin{aligned} \hat{E}(n) &= g^3 U_*^{-5} E(n) &&= \text{dimensionless spectrum level,} \\ \hat{n} &= U_* n/g &&= \text{dimensionless frequency,} \\ \hat{X} &= Xg/U_*^2 &&= \text{dimensionless fetch,} \\ \hat{T} &= Tg/U_* &&= \text{dimensionless duration.} \end{aligned}$$

In principle (28) then reduces to

$$\hat{E}(n) = \phi(\hat{n}, \hat{X}, \hat{T}) \quad (29)$$

ϕ being a universal function valid provided other forces, such as capillarity and viscous attenuation in the water are negligible.

4. DEVICES AND METHODS

In this section, we list some of the instruments and techniques which have been used, the spectra and ranges which they directly measure, and their limitations.

Wave Staffs and Spar Buoys

Electrical wave probes of two kinds have been used, namely resistive and capacitative. The probe in itself is typically of the order of a few mm or less in diameter, and capable of operating to very high frequency and short wavelength; it may be mounted on a tower fixed to terra firma, or alternatively deployed on a spar buoy, the design of which gives the spar an almost stationary characteristic to all but the very longest swell waves. A single probe gives $E(n)$. Arrays of probes may also be used, from which directional information may be inferred, notable recent experiments of the latter kind being those of Gilchrist (1966), using a line array and of Leykin and Rozenberg (1971), using both line arrays and planar arrays. One difficulty of using probes is that of dynamic range. The probe has to be long enough to include the highest waves, yet for acoustic applications, we require to measure very small waves riding on top of the main waves. This leads to limitations of signal-to-noise at high frequency, but can be alleviated by using prewhitening prior to recording, as was done for example by Kondo et al (1973) for recording from 0.1 to 30 Hz waves over a spectrum density range of 90 dB.

Motional Wavebuoys

Two types of motional wavebuoy, developed at the National Institute of Oceanography (England) have been particularly valuable in yielding excellent spectral and some directional information in the open ocean, being normally deployed from a ship. The pitch-roll buoy {Longuet-Higgins et al (1963)}, approximately 2m in diameter, measures local vertical acceleration, pitch and roll, which by analysis of auto, co and quadrature cross-spectra is capable to yield $E(n)$ or $E_1(k)$ with some directional information - that is a partially

CROWTHER: Surface wave spectra

resolved $E_{2D}(\underline{k})$, amounting to first 5 angular harmonics. The angular resolution is thus of order 100° depending on the window selected. The estimate of $E(n)$ is obtained only from the accelerometer and is thus direct, whereas the angular information requires the assumption of the dispersion laws for its extraction. The finite size of the buoy and accelerometer sensitivity limit its response to about $0.05 \lesssim f \lesssim 0.7$ Hz.

The Cloverleaf buoy {Cartwright and Smith} (1964) is effectively an equilateral triangle assembly of 3 pitch-roll buoys and measures wave curvature as well as slope and acceleration generating the first 9 angular harmonics. The angular resolution is finer because of the additional information, being of order 55° , but because of increased size, the frequency range is only $0.06 \lesssim f \lesssim 0.4$ Hz.

Line arrays of four single buoys have also been used, notably by Snyder and Cox. (1966) and Cartwright and Smith (1964).

Probe and Motional Wavebuoy

Crowther (1970, 1971) has used a combined motional and probe wavebuoy to assist in measurements of high frequency waves in the presence of large long wave components. The buoy was equipped with pitch-roll and acceleration at low frequency as is the NIO device, but in addition deployed a number of probes for high frequency measurements. The cross-over for vertical motion was in the vicinity of 0.4 Hz, and the upper limit for the probes was of order 10-15 Hz. As with the other wavebuoys, this device is operated from a ship at any point in the ocean required, but has the advantage of higher frequency coverage.

Remote Methods - Vertical

To these direct measures may be added a range of more or less remote techniques. Best developed of these are the use of high definition altimeters worked from aircraft, using either a radar beam {Barnett and Wilkerson (1967)}, or laser beam {Schule et al (1971)}. Beam widths limit these methods to rather long waves, about $\gtrsim 17m$ ($\lesssim 0.3$ Hz) for the laser technique, and combined with range resolution, which is only $\pm 0.15m$, to $\lesssim 0.15$ Hz for the radar beams.

Because of the relatively high speed of the aeroplane, these techniques measure effectively an almost time frozen surface, with some correction needed for relative wave-aeroplane motion. Results are usually obtained in a form of $E_{1D}(k_1)$ - a planar profile spectrum, although by making assumptions about the angular distribution, it is possible to convert to $E(n)$, to within an uncertainty of at most a factor of < 2 . The absolute accuracy and frequency range of these techniques are slightly lower than those of wave staffs or motional buoys, but their deployment flexibility has led to excellent studies of wave growth at different fetches.

The acoustic equivalent of the altimeter is the inverted echo-sounder. An example consisting of an array of such sensors given by DeLeonibus (1963) working at depth 80 ft, was capable of measuring spectra $E(n)$ between $0.04 < f < 0.45$ Hz, results being in close agreement with those found using the direct methods.

Remote Methods - Oblique Incidence

These are the least well developed of all at present, although for some purposes they have obvious advantages. 3 types have appeared in the literature, namely stereophotography, fourier transform photography, and radar scatterometry.

Early stereophotography {Coté et al (1960)} enabled directional information to be obtained at wavelengths from $\sim 200m$ to $20m$, $0.1 < f < 0.29$ Hz, with an $E(n)$ spectrum in some agreement with wave staff results. $E_2(\underline{k})$ spectrum was obtained by analysis of a grid of points in two dimensions.

More recently, Dobson (1970) has extended the stereo photograph to short range very high resolution studies, capable of measuring spectra at wavelengths from about $0.5m$ to $0.8cm$ $\{ \equiv 1.8 < f < 30 \text{ Hz} \}$. His technique uses planar profiles, and therefore measures $E_{1D}(k_1)$.

Another photographic technique which has recently been revived is the use of diffraction analysis of single photographs of the sea surface, exploiting

CROWTHER: Surface wave spectra

the Fourier transform property of optical diffraction to obtain slope spectra, approximating to the kind $S_{2,1,1}(\underline{k})$ {Stilwell and Pilon (1974), Stilwell (1969)}. The technique rests on the assumption of uniform illumination, a known reflectivity versus incidence angle law, with corrections for perspective distortion and the response of the photographic plate. The method is probably barely more than semi-quantitative at present, but the results of Stilwell and Pilon indicate at least the expected shape of the spectrum when converted to $E_{1u}(\underline{k})$ form, and order of magnitude agreement with the extrapolation from longer wave methods. The wavelengths measurable were ~ 30 cm to 5 cm. Although at present limited, the method is in principle less tedious than the stereophotographic, and covers similar wavelength ranges.

Valenzuela et al (1971) have attempted to measure sections of the spatial spectrum $E_{2U}(\underline{k})$ using backscatter of the U.S. Naval Research Laboratory's 4 frequency radar. This is an inverse problem, in that, having measured the backscatter, theoretical expressions for the latter in terms of $E_2(\underline{k})$ were then used to estimate $E_2(\underline{k})$, over wavelengths 0.7m (UHF at 30° incidence) to 1.8 cm (X band at 70° incidence), equivalent to surface frequencies of $1.5 < f < 13$ Hz. Two main doubts about the accuracy of this method have arisen, namely the theoretical validity and the equipment calibration accuracy.

As with photography, the main value is in studying high frequency waves, and we return to a discussion of both sets of results in Section 8.

Another EM technique which has found occasional use is the use of radio wave backscatter Doppler spectrum analysis {Crombie (1972), Barrick (1972)}. This technique is suited to longer waves, but cannot be used for shorter waves because of the modulation of their Doppler by the longer waves, a practical limit at $f \lesssim 0.35$ Hz seems to be indicated. Williams (1973) has used the acoustic variant of this technique, but using forward reflection rather than backscatter. The working wave frequency limit is similar. Both of these methods need to assume the dispersion laws. In principle they then measure the $E_{2D}(\underline{k})$ spectrum, or sections of it, although in practice, results are reduced to estimated $E(n)$ spectra.

5. WIND WAVE SPECTRUM GENERATION - INITIAL STAGES

The history of modern wave generation theory dates to the papers of Phillips (1957) and Miles (1957, 1959, 1960, 1961). These commenced as two different mechanisms, which may be summarized as follows. In Phillips mechanism, it is assumed that the wind flow is turbulent, consisting of advected pressure fluctuations, which act on the water surface to raise waves, the energy spectrum of which grows linearly with fetch and is directly related to the air pressure fluctuation spectrum. Theory predicts a maximum wave generation in directions usually away from the wind direction by an angle $\theta = \arccos(c/U)$. In Miles's calculation, the growth of an already established wave under the shear flow of the wind over its profile was considered, the initial calculation being based on a quasi laminar distortion of the basic logarithmic wind profile. It emerges that the wind wave coupling is proportional to the second derivative, d^2U/dz^2 , of wind profile, taken at that height where the air stream velocity just matches the wave phase velocity. This mechanism is relatively effective only for $25 \lesssim c/U_* \lesssim 10$. Outside these limits the matched layer is either too high for appreciable coupling for faster waves, or is within the laminar sub-layer, where $d^2U/dz^2 = 0$, for slow waves. However, both Miles (1960) and Phillips (1966) considered the additional generation due to turbulent flow effects in the wave induced air stream below the matched layer, allowing the possibility of efficient coupled wave generation some way outside the above limits, and also considered the two mechanisms as complementary. Put in simple terms, the combined mechanism predicts an initial growth of the spectrum according to a law

$$\frac{d}{dT} E = \frac{\partial}{\partial T} E + \underline{v} \cdot \nabla E = \alpha + \beta E, \quad (30)$$

$E = E_{2D}(\underline{k}, T, X)$, $\underline{v} = \underline{v}(\underline{k})$ being group velocity, α representing the Phillips forcing term, and β representing the Miles amplification term. Under steady wind conditions, $dE/dT = \underline{v} \cdot \partial E / \partial X$, and $\partial E / \partial T = 0$, so that we expect, for a given wave component, a growth versus fetch of

$$E = (\alpha/\beta) \{ \exp (\beta X/v) - 1 \}, \quad (31)$$

where the values of α , β depend of course upon the frequency and windspeed.

Experimental field studies, by Snyder and Cox (1966), Barnett and Wilkerson (1967) and Schule et al (1971) have demonstrated the essential correctness of this mixed forced and coupled growth mechanism. DeLeonibus and Simpson (1972) have demonstrated the correctness of the model also in duration-limited conditions. Fig. 1 shows some collected experimental results, clearly indicating the initial linear and subsequent exponential growth.

Both the α and β terms found experimentally tend usually to exceed the values computed from theory - although for α this may be due to lack of reliable information on the turbulent pressure spectrum over the sea. Analysis of experimental results is simplified usually in that (30) is applied to $E(n)$ spectra, whereas theory implies that α and β are functions of the angle between the wind direction and \underline{k} , so that omnidirectional spectra are inadequate. Nevertheless, an empirical fit by Inoue (1966) to available data, for the β term, shown in Fig. (2), does agree to order of magnitude with the Miles-Phillips theoretical curve, the plot used being the dimensionless one of β/f vs $\hat{n} = U_*/c$.

Barnett (1968) has proposed a simpler empirical form for β of:

$$\beta = 5s f \{ (U/c) \cos \theta - 0.9 \}, \quad (32)$$

$$\{ = 0 \text{ if } (U/c) \cos \theta - 0.9 < 0 \}$$

where s = air/water density ratio, θ = angle between wind and wave component direction, and an empirical form for α as

$$\alpha = \pi P(\underline{k}, n) g k \rho^2 c^2 \quad (33)$$

$$P(\underline{k}, n) = \frac{6.13 \cdot 10^{-4} U^4}{\pi n^2} \{ v_2 / (v_2^2 + k^2 \sin^2 \theta) \}.$$

$$\cdot \{ v_1 / (v_1^2 + \overline{k \cos \theta - H^2}) \} \quad (34)$$

Eqn. (33) is the form given by Phillips, where $P(\underline{k}, n)$ is the air pressure spectrum, ρ = water density, $v_1 = 0.33 H^{1.28}$ (Mks) $v_2 = 0.52 H^{0.92}$ (Mks),

$H = n/U$ (Mks). Collins (1972) showed that at least the experimental results of Snyder and Cox for $\theta = 0$ can be fitted quite well by using (32-34) {see Fig. 1 in Part }, although it is questionable theoretically whether the supposed total cut-off in β for low frequency waves is quite correct.

6. NON-LINEAR INTERACTION

As the wave spectrum energy builds up to approach equilibrium, equation (30) ceases to hold, owing to non-linear effects. These are of two kinds, non-conservative wave breaking and conservative wave-wave generation. The former is important in controlling the level of the equilibrium spectrum, but has received virtually no detailed theoretical treatment; the latter is more theoretically tractable. Investigations by Phillips (1960), Hasselmann (1962), Longuet-Higgins (1962) Benny (1962) and others have shown that secular wave-wave generation effects will appear only at third order for gravity waves and therefore to generate wave energy at \underline{k} requires the interaction of three wave components, at say $\underline{k}_1, \underline{k}_2, \underline{k}_3$. The strength of interaction is thus proportional to the cube of the mean square surface slope. A review of work on non-linear interaction with a further bibliography is contained in Hasselmann (1968), whilst the importance of non-linear interactions in re-distributing the spectrum energy has been carefully analysed using experimental data gathered in project JONSWAP by Hasselmann et al (1973). Fig. (3) is taken from the latter paper, and shows the calculated rate of change of spectrum for an average experimental fetch limited spectrum owing to non-linear interactions, with certain assumptions about angular distribution. The general effect is that wave components at frequencies between just above the spectral peak and about twice the peak frequency lose energy to frequencies below and above this band. The gain at low frequencies appears to be in part responsible for the progressive growth of the spectrum, whilst the flow of energy towards the high frequencies must largely be lost afterwards by dissipation, since those frequencies are usually 'saturated'.

For the example given, in the vicinity of the peak we have $\left| 2\pi \frac{dE}{dt} (n) \right|_s$

$1.7 \cdot 10^{-5} \text{ m}^2$, whilst $2\pi E(n) \lesssim 0.22 \text{ m}^2 \text{ s}$, at $f \sim 0.3 \text{ Hz}$; thus to order of magnitude, we have a non-linear rate of change of $\beta^1/f = \left| \frac{dE/dt}{E \cdot f} \right| \sim 0.25 \cdot 10^{-3}$. Comparing this with Fig. (2), we see that non-linear action is apparently about one order of magnitude weaker than the shear flow instability ($\beta/f \gtrsim 2 \cdot 10^{-3}$) for fetches at which the spectral peak is at frequencies travelling more slowly than the wind, $U_*/c \lesssim 30$ say, although for longer fetches, it appears that non-linear forces could take over the generation of wave components travelling appreciably faster than the wind, where the shear flow force is small. Conversely, for the Fig. (3) at higher frequency $2\pi dE/dt \sim 8 \cdot 10^{-7}$ at $f = 1 \text{ Hz}$, where $2\pi E(n) \sim 5 \cdot 10^{-4}$, so that $(dE/dt)/Ef \sim 1.6 \cdot 10^{-3}$ at 1 Hz, which indicates that non-linear energy supply is comparable with shear flow at high frequencies, for an appropriately established spectrum.

7. LATER GROWTH AND THE EQUILIBRIUM SPECTRUM

The concept of the equilibrium spectrum is due to Phillips (1958), who proposed that there would be a section of $E(n)$ where waves were fully developed, in that wave breaking would set a limit to any further growth. With a sufficient energy input, the spectrum in this region should then be approximately independent of windspeed and fetch, and be controlled only by gravity. On dimensional grounds, it can then be seen that the only possible form for this saturated section of the spectrum in the gravity regime is:

$$E_1(k) = \frac{1}{2} a k^{-3}, \quad (35)$$

$$E(n) = a g^2 n^{-5} \quad (36)$$

where a is a dimensionless constant. The approximate validity of (36) over an appropriate frequency band, typically from ~ 1.5 times the spectrum peak frequency to $\sim 2 \text{ Hz}$, has been demonstrated by numerous observations, the value of a varying between about 0.7_{10}^{-2} and $1.1 \cdot 10^{-2}$ for open-ocean measurements.

An extension of this saturation regime is that of a complete equilibrium spectrum, to which the spectrum tends at sufficiently long fetch. Many theoretical

forms for this 'fully developed' spectrum have been proposed, the most recent for $f \lesssim 2$ Hz being that of Pierson and Moskowitz (1964), in the form

$$E(n) = ag^2 \exp \{-b(c/U)^4\} \quad (37)$$

where $a = 8.1 \cdot 10^{-3}$ $b = 0.74$. The strict correctness of the concept of a limiting spectrum has been questioned, and in view of recent discoveries in non-linear growth, it does not seem to be necessary that the whole spectrum should cease to grow at any limiting point. Nevertheless, in practice the Pierson-Moskowitz spectrum is of some usefulness in approximating experimental results at very long fetches. The peak of the Pierson-Moskowitz spectrum occurs at $n = n_{\max}$ such that $g/n_{\max} = c(n) \sim 1.14 U$, a wave travelling just faster than the wind.

One interesting effect which violates the idea of a rigidly controlled saturation level is that of overshoot of the spectrum, which was first observed at sea by Barnett and Wilkerson (1967), and has subsequently been confirmed by Schule et al (1971), DeLeonibus and Simpson (1972) and Hasselman et al (1973) in the open sea, and by Sutherland, and Mitsuyasu (1969) in laboratory conditions. On a microscopic level at sea, the overshoot effect has been observed at wavelengths of order 10 cm as a result of wind gusts by Stilwell and Pilon (1974). The effect is that in a non-equilibrium sea, a wave spectrum component will continue to grow to a level of \sim twice the equilibrium level, before subsequently falling back to the latter. There is some evidence for subsequent undershoot {Barnett and Sutherland (1968)}. The overshoot effect is just visible in Fig. (1c) for a single frequency and is clearly visible in Fig. (4) after Hasselmann et al (1973). The explanation for overshoot, qualitatively at least, would appear to be that for wave components close to the spectrum peak both their conservative non-linear spectrum flux and the non-conservative loss by breaking depend critically on the presence or absence of waves of slightly lower frequency. In the absence of such longer waves, as one has at the appropriate fetch, the spectrum level will grow to a point where the longer waves start forming appreciably, whereat the energy flux becomes strongly negative, and

the spectrum level approaches equilibrium. Thus, the spectrum peak frequency will reduce with increasing fetch. This is shown in a dimensionless compiled plot, taken from Hasselmann et al (1973), which also shews the Pierson-Morkowitz value. It appears to be an open question whether the power law trend for n_{\max} would continue beyond the latter, or truly reach a steady state. Similar results were found by Volkov (1968).

There is also evidence that the value of the equilibrium constant is not strictly independent of windspeed and fetch. This is not surprising, if we remember that dissipation by wave breaking will increase with increase of mean square surface acceleration $\int n^4 P(n)dn$, which, for constant a , would increase logarithmically as the peak frequency reduces. This problem has been investigated by Longuet-Higgins (1969), who shewed that the functional energy loss per mean wave period by breaking would be of order $\exp(-1/8a)$, so that for a given energy supply, as the total energy builds up with increasing fetch, a would have to reduce slightly, thus:

$$a = \{D \log_{10} (g X/U_*^2) - G\}^{-1}, \quad (38)$$

where D , G are dimensionless constants. Mitsuyasu (1969), analysing laboratory, reservoir, bay and ocean data, has found an empirical fit using $D = 21$, $G = 34.5$ as shown in Fig. (6). For open ocean conditions, variations in a remain fairly small, even for quite large variations in dimensionless fetch.

Related to this variation in a with \hat{X} and to non-linear forces spreading the spectrum energy is the fact that at very low windspeeds, or where the wind drops in the presence of an already formed sea, the n^{-5} law often still appears to hold, but with a reduced constant. Ewing (1969) shews a result with n^{-5} at $a \sim 1.2 \cdot 10^{-3}$ for $U \sim 0$ in a falling sea, whilst Crowther and Perry (1970) shew low windspeed long fetch spectra having $a = 1.7 \cdot 10^{-3}$ for $U = 1\text{m/s}$, $a = 3.6 \cdot 10^{-3}$ for $U = 1.5\text{m/s}$.

8. HIGH FREQUENCY SPECTRA

Pierson and Stacy (1973) have proposed that the concept of a fully developed spectrum, as embodied in the Pierson-Moskowitz form, can be extended

beyond the frequencies commonly measured at sea, suggesting 4 further frequency regimes where different power laws should apply. Experimentally, however, there appears to be much more variability in high frequency spectra than there is in the Phillips regime, and it is very doubtful that laboratory measurements, on which much of the higher regions of Pierson and Stacy's spectrum rely, can be applied in sea spectra. We may conveniently define the high frequency portion of the spectrum as being from about 2-13 Hz for gravity waves (0.4-0.02m wavelength) and beyond 13 Hz for capillary waves. Direct experimental studies of the h.f. wave spectrum in the sea are due to Crowther and Perry (1970), using a probe mounting surface wavebuoy in the open sea at frequencies ≤ 13 Hz, Leykin and Rozenberg (1970), at $f \leq 7$ Hz, using a fixed probe at 50m from the shore in 15m depth, Kondo et al (1973) using a fixed probe at 1 km from the shore in 20m depth at frequencies up to 33 Hz, Kinsman (1960) using a probe in a bay at $f \leq 2.5$ Hz, and Garrett (1969) using fixed probes at 8 km fetch at up to 3 Hz. To these may be added the photographic work of Dobson (1970) at wavelengths down to ~ 1 mm, and the radar backscatter of Valenzuela et al (1971), at wavelengths 2-70 cm.

The first thing which is evident about high frequency E (n) spectra is their large variability with conditions. Some collected results are shown in Fig. (7), where it is clearly evident that compared with 1 Hz, say, the variability in the spectrum at 2-10 Hz is large, and increases with frequency. This is consistently apparent in all sea results, but is not found to the same extent in laboratory results analysed by Pierson and Stacy (1973). Secondly, there is a general tendency for the spectrum to exceed the Phillips formula, the power law being n^{-m} , where $2.5 < m < 4$ depending on the sea state and frequency band examined. There is a general tendency for the spectrum level to increase with increasing windspeed, but the correlation is very imperfect. The results of Kondo et al (1973) suggest a possibly closer correlation with surface wave height, $H_{1/3}$.

This region has been examined by Pierson and Stacy (1973), using only Kinsman's and Leykin and Rozenberg's results, supported by laboratory experi-

ments, making the explicit assumption that high frequency spectra depend only on local windspeed, since the fetch required for their generation is very short. On this basis, they suggested the existence of a so-called Kitaigordskii regime with n^{-4} dependence, and a transitional regime with rather uncertain dependence on n , leading to a capillary wave regime. The theoretical basis of the Kitaigordskii n^{-4} regime was that of turbulence generation when proposed {Kitaigordskii (1962)}, but in view of more recent studies, non-linear action and shear flow seem quite capable of delivering sufficient energy to these wavelengths, and there does not seem to be any obvious reason why the Phillips law should not hold at frequencies up to the onset of the capillary regime, say $f \lesssim 10$ Hz. Also the assumption of local wind dependence only is strongly denied by the experimental results.

To this complication in the $E(n)$ spectra must be added the fact that Dobson's photographic work does not shew nearly so large a departure from the Phillips k^{-3} law, as do the $E(n)$ spectra from the n^{-5} law, as is shown in Fig. (10), where photographic $E_{1U}(k)$ spectra, as such they must be supposed to be, appear to be closely related to much lower frequency spectra, using a Phillips constant of $a = 8.1 \cdot 10^{-3}$ if we assume an omnidirectional spectrum, for which $E_{1U}(k_1) \sim \frac{1}{2} E_1(k)$ for k^{-3} dependence. Other results by Dobson shew some increase relative to this level, and the accuracy of measurement appears to be only to within a factor of ~ 2 , but the power law still appears close to k^{-3} . The radar backscatter of Valenzuela et al (1971) also shews a very close approximation to a Phillips k^{-4} law for $E_2(k)$, although there are uncertainties of definition and calibration in these experiments which make the absolute level unreliable, as shewn by Pierson and Stacy (1973). Even taking these into account however, these results also point to a k spectrum much closer to the Phillips law than are the measured $E(n)$ at sea. $E(n)$ spectra measured in the laboratory by Sutherland and others, as analysed by Pierson and Stacy, appear to lie at levels below those measured in the sea.

It appears that a simple fact has been overlooked which might explain all these discrepancies. This is that as n, k increase, the phase velocity reduces, whereas in the open sea these short waves will be 'riding' on the larger waves. There will be a value of n such that the surface particle velocity will be significant compared with $c(n)$, whereupon the $E(n)$ spectrum will become distorted by random Doppler modification owing to surface particle velocity. Numerically, we can estimate where this is likely to occur as follows. Distortion in $E(n)$ will probably be severe at a frequency n , such that

$$c(n_1) \approx \sigma_{pvh}, \quad (39)$$

where σ_{pvh} is the r.m.s. horizontal particle velocity. For deep water σ_{pvh} is given by

$$\sigma_{pvh}^2 = \int n^2 E(n) dn, \quad (40)$$

which for a Pierson-Moskowitz spectrum implies

$$\sigma_{pvh} \approx 0.065 U, \quad (41)$$

So that the critical frequency is

$$f_1 = n_1/2\pi \sim 24/U \text{ (Mks)} \quad (42)$$

For a windspeed of order 10 m/s, we shall expect pronounced effects by frequency ~ 2.4 Hz, which is just about the frequency region where the upper curves in Fig. (7) start departing from Phillips.

Asymptotically, at high sea states and high frequencies, we could suppose a limiting regime where $\sigma_{pvh} \gg c(n)$, so that the high frequency waves are approximately static, being convected across the probe by the particle velocity. Under these conditions, we may apply a dimensional argument to estimate the asymptotic form of $E(n)$ as follows. Suppose a spatial spectrum

$E_1(k) = \frac{a}{2} k^{-3}$ obeying Phillips law, $E(n)$ must then depend asymptotically only on n , σ_{pvh} and a , to which it must be proportional, we therefore obtain the only possible dimensionally correct form

$$E(n) \approx d \cdot a \sigma_{pvh}^2 n^{-3}, \quad (43)$$

d being a dimensionless constant, presumably of order of magnitude unity. For the Pierson-Moskowitz fully developed sea:

$$E(n) \approx 3.4 \cdot 10^{-5} d \cdot U^2 n^{-3} \text{ (P.M.)}, \quad (44)$$

predicting n^{-3} spectrum proportional to U^2 .

This n^{-3} spectrum appears fairly well confirmed by the results of Crowther and Perry (1970) and Kondo et al (1973). The u^2 law is not obeyed precisely, because real sea states are rarely fully developed, but for those results in Crowther and Perry (1970) coming closest to fully aroused conditions, a mean value of $d \approx 4.1 \pm 2$ has been found against Eq. (44). Theory implies less scatter if $E(n)$ is plotted against σ_{pvh}^2 . The latter was computed using (40) for the spectra of Crowther and Perry, and specimen plots are shown in Fig. (8), compared with the windspeed plot. Much less scatter is evident against σ_{pvh}^2 than against U^2 - for example at 7Hz the correlation coefficient between $E(n)$ and σ_{pvh}^2 is 0.944, but only 0.705 for $E(n)$ and U^2 . This supports the Doppler mechanism as opposed to local windspeed effects. The average value estimated from these results against σ_{pvh}^2 at $f \leq 10$ Hz is $d = 3.7 \pm 1$, using $a = 9 \cdot 10^{-3}$, in close agreement with that estimated against U^2 for the most developed seas. The results of Kondo et al strongly suggest less scatter against σ_{pvh}^2 but they do not admit of calculating the latter. It is possible that the estimate of d made above is somewhat too small, in that the wavebuoy used will to some extent follow the horizontal motion of the longer waves, thereby reducing the Doppler, but the extent of this effect is not well known. This could explain the fact that the $E(n)$ of Kondo et al tend to exceed those of Crowther and Perry. Fig. (9) shows the Kondo spectral levels versus U , with (44) superposed at $d = 4.1$.

The general u^2 and n^{-3} laws appear well obeyed, at least in the gravity regime. The Leykin-Rozenberg results tend to fall slightly below (44) at $d = 4.1$. If significant, this result could be owing to the proximity of the shore at 80m.

9. DISPERSION LAWS

The argument in the last section denies the validity of the dispersion laws at high frequency in the sea, but what of experimental tests? Not much information is available, but a test at lower frequencies has been made using results of pitch-roll wavebuoy studies, where we should have $S(n) = k^2(n) E(n)$, enabling $k^2(n)$ to be compared with the ratio S/E {Longuet-Higgins et al (1963)}. Such comparisons indicate that not much departure from $n^2 = kg$ occurs at $f \leq 0.7$ Hz. A similar test has been made by Grose et al (1972) using a triangular probe array and working over 0.25 - 0.61 Hz, analysing results using an empirical relation

$$n^a = b k(n) , \quad (45)$$

in place of (1), where a, b are constants determined by best fit to $k(n)$ found by the slope/ elevation spectra ratio. Values of $1.2 < a < 2.05$, $4 < b < 11$ Mks were found, containing the classical $a = 2$, $b = 9.81$. Fluctuations in a, b were found to correlate from run to run, with regression law $b = -5.42 + 7.53a$ (Mks). This is evidently not so much a true physical effect but a consequence of the system of units used, since the mean n in the range is $\bar{n} = 2.7$ rad/sec it follows that purely random fluctuations in the apparent power law, a , due to experimental indeterminacy would require strongly correlated variations in b to enable the classical law to hold approximately within the band. The correlation of a and b would have been much less had the authors tried fitting in a different system of units, e.g. to $(n/\bar{n})^a = bk(n)$. For the majority of points quoted, the classical law holds near the centre of the band, and since there is nothing special about this band, we may suppose that the major effect is simply due to experimental fluctuations in finite samples distorting the apparent power law over a relatively narrow band of observation. Nevertheless, there is a slight trend for $a < 2$ on average. This may be due to slight non-linearity effects at the upper end of the band. Note that the asymptotic effective $n(k)$ law for

high frequencies following the Doppler hypothesis in section 8 would be a linear one ($a \sim 1$), so that it is possible that the $a < 2$ trend at lower frequencies marks a slight onset of Doppler distortion, although the frequency is lower than that where such effects would be predominant.

An alternative approach to testing the dispersion laws was made by Crowther (1971), who compared measured spatial correlation with that computed from measured $E(n)$ spectra. Within the limitations of the test, departures from the assumption of classical dispersion were found to be statistically insignificant. This test was however performed broad band, where it could be shown that the dominant wavelength in influencing the spatial correlation at the shortest usable separation was of order $\lambda \sim 4m$ - say $f \sim 0.6$ Hz, where no great departure from classical dispersion would be expected.

Leykin and Rozenberg (1971) reported measurements using a 2-dimensional array in the vicinity of 6 Hz, with spectra indicating an approximate obedience to the dispersion law, but the sea state was reported to be very low - windspeed ~ 1 m/sec.

10. DIRECTIONAL DISTRIBUTION

Directional information has been obtained using the pitch-roll wave-buoy {Longuet-Higgins et al (1963)} and using the Cloverleaf wavebuoy {Cartwright and Smith (1964)}. In the first case, the directional distribution was assumed to follow a law

$$E_{2D}(k, \theta) = E_{2D}(k, 0) \{ \cos(\theta/2) \}^{2s} (U/c), \quad (46)$$

θ being angle away from the downwind direction, and values of the coefficient s were obtained from comparing angular harmonics. For Cartwright and Smith's results an effective beamwidth can be estimated at the half power point of the measured angular distributions, from which s may be estimated. The combined results are shown in the form of s versus U/c , using $u \approx 27U_* = 27K U_1$ to convert from Longuet-Higgins's plot. There appears to be consistency between the two observations. s falls rapidly with increasing frequency. A least

squares regression fits the measured results by the form;

$$S \approx 11 \exp(-0.7 U/c), \quad (47)$$

quite satisfactorily.

Measurements of angular distribution have also been obtained from Project SWOP {Coté et al (1960)}, by Gilchrist using a probe array in fetch limited conditions (1966), by Krylov et al (1968), by Leykin and Rozenberg (1971), and Hasselmann et al (1973). The form of analysis by Coté et al was in terms of a limited number of less flexible angular terms, but is in broad agreement with the wavebuoy results. Gilchrist's results were fetch limited in a complex way, and serve more as a lower limit measurement of broadening. On this basis they confirm the long fetch wavebuoy results. They also appear to show support for the Phillips mechanism and 'resonant' angle at short fetch, in that measured peaks were offset from the wind direction. Krylov et al modelled angular distributions using a $\{\cos(\theta)\}^p$ form, it being assumed that there are no waves travelling against the wind ($|\theta| > \pi/2$). Allowing for the estimated windspeed from their spectral peak, their formula for p appears to be $p \sim 2 U/c$, which is of similar width to (47) near the spectrum peak, $\sim 80^\circ$ width between half power points, but with less broadening at higher frequencies. Hasselmann et al made measurements of width in growing conditions, where they found a somewhat narrower width near the local spectrum peak than this. It is also not certain whether the angular width should more closely be regarded as a function of U/c , or of n/n_{\max} , n_{\max} being the local spectrum peak. The Hasselmann et al paper suggests the latter, in which case if (46) is converted assuming a Pierson-Moskowitz spectrum for the wavebuoy measurements, we might expect

$$S \approx 11 \exp(-0.61 n/n_{\max}), \quad (48)$$

Although Hasselmann et al are then only at about 2/3 the broadening predicted in the region of spectral peak. A possible reason for this might be the further broadening of long fetch by non-linear interaction.

11. SUMMARY

We have attempted to review significant progress over the last 15 years, clarifying the different types of spectra measured, and trying to emphasize the acoustically most significant part of the spectrum. Spectra at frequencies $\lesssim 1$ to 2 Hz and their growth and non-linear interactions appear to be fairly well understood. The Phillips saturation spectrum at the frequencies $\lesssim 1.5$ times peak frequency is very well established, with a constant of $a = 0.007$ to 0.01 in the open ocean, although it appears that it does vary slowly with fetch, in the way expected theoretically. The details of the non-equilibrium spectrum in the vicinity of the spectrum peak are more complicated than supposed in earlier wave generation theories, and the phenomenon of an overshoot to order twice the equilibrium spectrum level in growing seas is well established, and at least partially understood. Directional information is also available in part, and shews that longer waves are more narrowly distributed over angle than are shorter waves, which appear to approach isotropy at least over $|\theta| < \pi/2$.

$E(n)$ above ~ 2 Hz tends to exceed the Phillips saturation form in a complicated way, which is partially correlated with windspeed but apparently dependent also on general roughness, in particular on mean square water motion. An explanation for this, departing from the conjectures of Pierson and Stacy and Kitaigorodskii, has been given here on the assumption of Doppler effect due to longer waves breaking the dispersion law connecting spatial and temporal spectra. This explanation appears to be consistent with the following facts: (a) that a departure from the Phillips $E(n)$ occurs well below the capillary frequency, at about the frequency predicted; (b) the departure correlates more closely with water motion than with local windspeed; (c) that high frequency $E(n)$ spectra at sea appear to exceed those measured in the laboratory, because of the absence of longer waves in the latter case; (d) that the spatial spectra in this region which may be estimated from

photography and radar backscatter appear to be closer to the Phillips law than do the temporal spectra.

The implication of this Doppler distortion at high frequencies for acoustic scattering is that the $E(n)$ spectrum will tend to over-estimate the spatial roughness spectrum very considerably. $E(n)$ ceases to be a good way of measuring the spectrum at $f \gtrsim 2$ Hz. One should measure spatially, although photographic methods are tedious and less well calibrated than direct methods, and radar backscatter appears at present to have similar disadvantages. One possible solution would be the use of a finely balanced array of probes at close spacing, processed to obtain the spatial correlation over say 0-50 cm, probably with frequency filtering to remove the effect of the longer waves. Such a correlation function could then be transformed to an $E_{1u}(k_1)$ or $E_2(\underline{k})$ spectrum, and compared with the Phillips spectrum and the supposedly anomalous $E(n)$ spectrum.

REFERENCES

T.P. Barnett

J. Geophys. Res. 73 513-530 (1968).

T.P. Barnett and A.J. Sutherland

J. Geophys. Res. 73 (22) 6879-85 (1968)

T.P. Barnett and J.C. Wilkerson

J. Marine Res. 25 (3) 292-328 (1967)

D.E. Barrick

Proc. I.E.E.E. Conference, Newport R.I. 'Ocean 72', (1972), p186-191

V.J. Cardone

Specification of the wind distribution in the marine boundary layer for wave-forecasting 'New York Univ. Geophys. Sciences Lab. Report TR-69-1 (1969).

D.E. Cartwright and N.D. Smith

"Buoy Techniques for Obtaining Directional Wave Spectra", from Buoy Technology, Marine Technology Soc., Washington (1964). p112-121

J.I. Collins

J. Geophys. Res. 77 (15) 2693-2707 (1972).

L.J. Cote et al

"The Directional Spectrum of a Wind Generated Sea" New York University, Meteorology paper 2 (6) (1960).

D.G. Crombie

Proc. I.E.E.E. Conference Newport R.I. "Ocean 72" (1972), p174-179

P.A. Crowther

"Calculation of Acoustic Backscattering from the Sea Surface from in-situ wave data", Unpublished Report (1971).

P.A. Crowther and I.R. Perry

"Measurements of Sea Surface Roughness Statistics for Various Windspeeds" Unpublished Report (1970).

E.L. Deacon and E.K. Webb

'Small Scale Interactions', in 'the sea' (ed. M.N. Hill) Vol. 1, pp 43-87, New York: Interscience.

P.S. DeLeonibus

'Ocean Wave Spectra,' pp 243-50, Englewood Cliffs, N.J., Prentice-Hall, INC. (1963).

P.S. DeLeonibus and L.S. Simpson

J. Geophys. Res. 77 (24) 4555-69 (1972).

E.B. Dobson

J. Geophys. Res. 75 (15) 2853-56 (1970)

J.A. Ewing

J. Marine Res. 27 (2) 163-171 (1969).

J. Garret

J. Marine Res. 27 (3) 273-77 (1969)

A.W.R. Gilchfist

J. Fluid. Mech. 25 (4) 795-816 (1966)

P.L. Grose, K.L. Warsh, M. Garstang

J. Geophys. Res. 77 (21) 3902-6(1972)

K. Hasselmann

J. Fluid Mech. 12, 481 (1962)

K. Hasselmann

'Weak interaction theory of Ocean Waves', in Basic Developments in Fluid Mechanics, New York, Academic Press, pp 117-182 (1968).

K. Hasselmann et al

Measurements of wind-wave growth and swell decay during the joint North Sea Wave Project (JONSWAP) Deutsche Hydrog. Z. 8(12), 1 (1973).

T. Inoue

"On the Growth of the Spectrum of a wind-generated sea according to a modified Miles-Phillips mechanism and its application to wave forecasting" New York Univ. Dept. of Meteorol and Oceanog. Rept. TR 67-5 (1967)

B. Kinsman

'Surface waves at short fetches and low windspeed', Chesapeake Bay Inst., Johns Hopkins Univ, Report No. 19 (1960).

S.A. Kitaigorodskii

Bull. Acad. Science, U.S.S.R. Geophys. Ser. No., (1) pp 73-80 (Eng. Trans.) (1962).

J. Kondo, Y. Fujinawa, G. Naito

J. Phys. Oceanog. 3, 197-202 (1973).

Y.M. Krylov, S.S. Strekalov, V.F. Tsypukhin

Sov. Phys. tzv. Atmos. and Oceanic Phys. 4(6)376-81 (1968) (Eng. Trans.)

M.S. Longuet-Higgins

J. Fluid Mech. 12, 321-32 (1962)

CROWTHER: Surface wave spectra

M.S. Longuet-Higgins

Proc. Roy. Soc. A, 310, 151-159 (1969)

M.S. Longuet-Higgins, D.E. Cartwright and N.D. Smith

'Ocean Wave Spectra' pp 111 - 131, Englewood Cliffs, N.J. Prentice-Hall, Inc. (1963).

J.W. Miles,

J. Fluid Mech. 3, 185 (1957), 6 568-82 (1959),
7, 469 (1960), 10, 496 (1961), 13, 433-48.

H. Mitsuyasu

'On the Growth of the spectrum of wind generated waves (2), Kyushu Univ. Res. Inst. for Appl. Maths. Rept. 59, 17, 235 (1969).

O.M. Phillips

J. Fluid Mech. 2 (5) 417 (1957)

O.M. Phillips

J. Fluid Mech. 4 (4) 426 (1958)

O.M. Phillips

J. Fluid Mech. 9, 193 (1960)

O.M. Phillips

'The Dynamics of the Upper Ocean' Cambridge Univ. Press (1966).

W.J. Pierson and L. Moskowitz

J. Geophys. Res. 69 (24) 5181 (1964)

W.J. Pierson and R.A. Stacy

'The Elevation Slope and curvature spectra of a wind roughened sea surface"
NASA Contractor Rept. NASA CR-2247 (1973).

J.J. Schule, L.S. Simpson, P.S. DeLeonibus

J. Geophys. Res. 76 (18), 4160-71 (1971).

P.A. Sheppard

Quart. J. Roy. Met. Soc. 84, 205-224 (1958)

R.L. Snyder and C.S. Cox

J. Marine Res. 24, 141-178 (1966)

D. Stilwell

J. Geophys. Res. 74 (8) 1974-86 (1969)

D. Stilwell and R.O. Pilon

J. Geophys. Res. 79 (9) 1277-84 (1974)

G.R. Valenzuela, M.B. Laing and J.C. Daley

J. Marine Res. 29(2) 69-84 (1971)

Y.A. Volkov,

Izv. Acad. Science USSR Atmos and Oceanic Phys. 4, 555-564 (1968) (Eng. Trans.)

R.G. Williams

J. Acoust. Soc. Amer. 53 (3) 910-20 (1973).

INITIAL GROWTH RATE

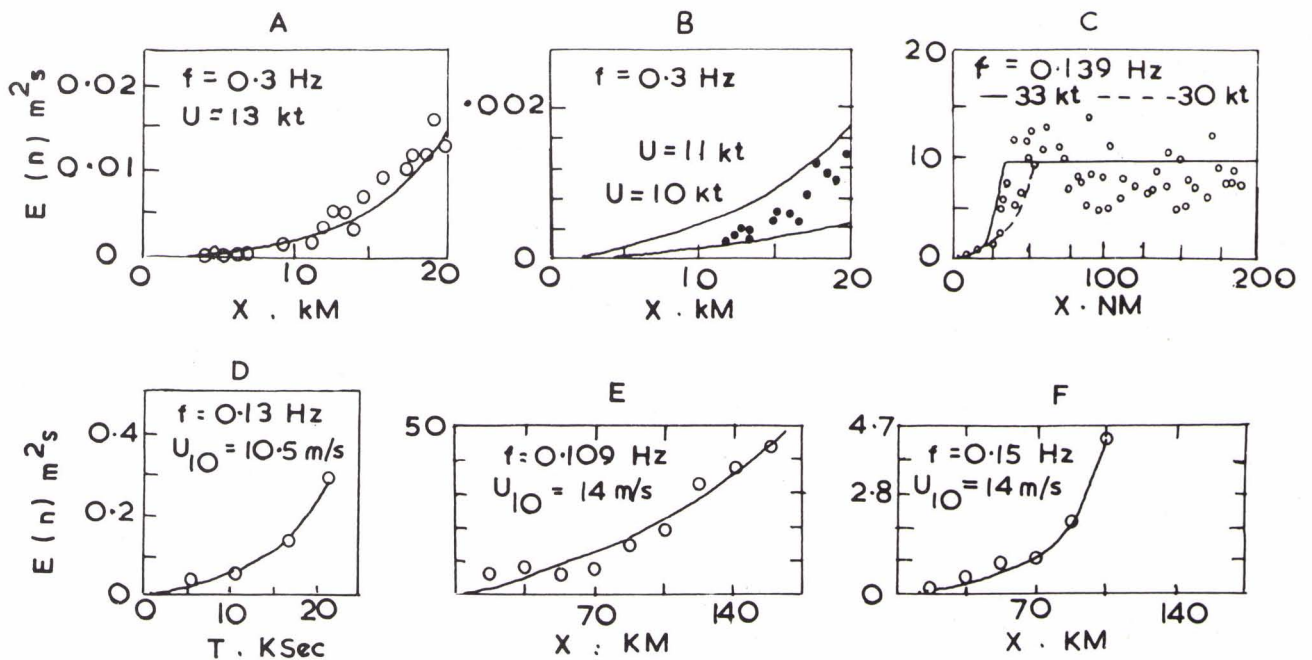


FIG. 1 SPECTRUM LEVEL GROWTH; (a,b) EXPTS. OF SNYDER AND COX, FITTED TO THEORY BY COLLINS (1972); (c) AFTER BARNETT AND WILKERSON; (d) AFTER DeLEONIBUS AND SIMPSON UNDER DURATION LIMITED CONDITIONS; (e,f) AFTER SCHULE ET AL (1971)

FIG. 2
 COUPLED GROWTH COEFFICIENT, EXPERIMENTS
 AND THEORY COMPARED, AFTER
 DeLEONIBUS AND SIMPSON (1972),
 EXPERIMENTAL POINTS:
 ● INOUE (1967); ○ BARNETT AND WILKERSON (1967);
 × SNYDER AND COX (1966);
 ▲ SCHULE, SIMPSON AND DeLEONIBUS (1971);
 ▽ DeLEONIBUS AND SIMPSON (1972).

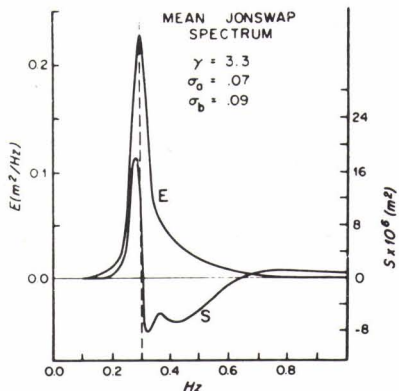
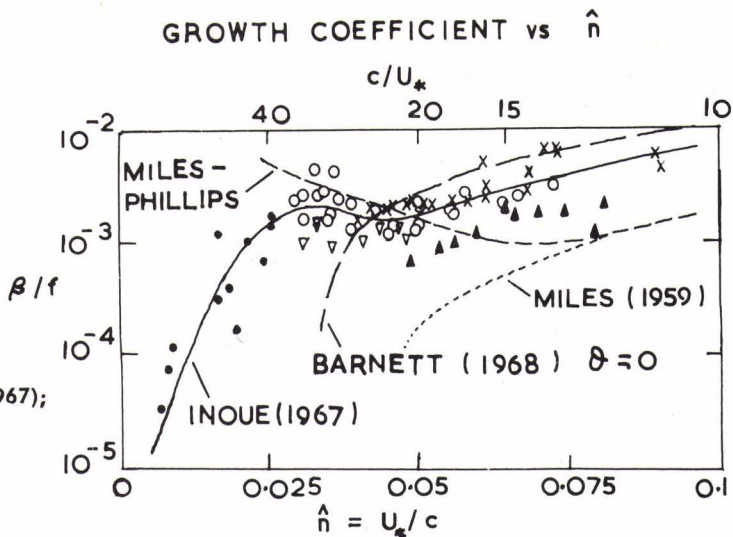


FIG. 3
 JONSWAP AVERAGE ENERGY SPECTRA AND COMPUTED NON-LINEAR
 RATE OF TRANSPORT OF ENERGY SPECTRUM.
 NOTE: $E(f) = 2 \pi E(n)$. FROM HASSELMANN ET AL (1973)

SPECTRUM EVOLUTION vs FETCH

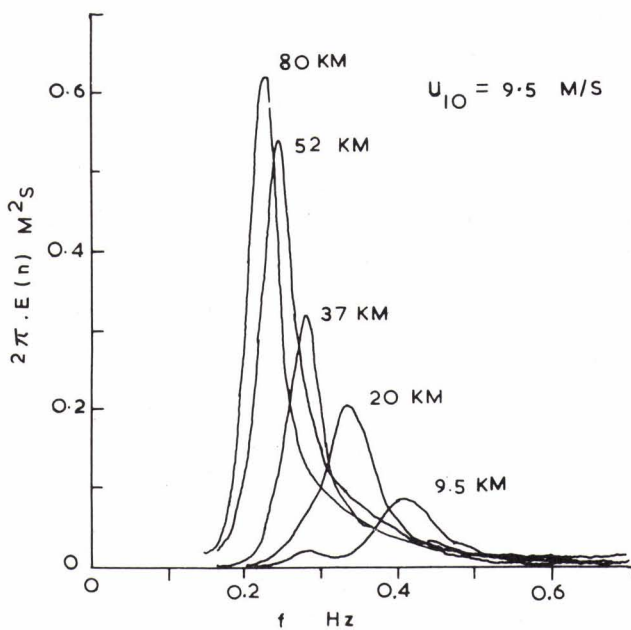


FIG. 4
 JONSWAP SPECTRAL GROWTH VERSUS FETCH,
 AFTER HASSELMANN ET AL (1973).
 THE OVERSHOOT EFFECT IS CLEARLY VISIBLE

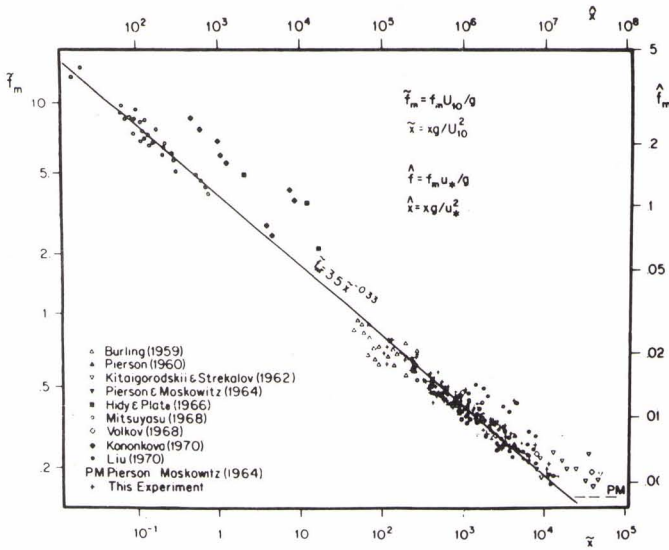


FIG. 5
DIMENSIONLESS PEAK FREQUENCY VERSUS
DIMENSIONLESS FETCH, COMPILED EXPERIMENTAL
VALUES FROM HASSELMAN ET AL (1973)

FIG. 6
PHILLIPS CONSTANT VS. FETCH, AFTER
MITSUYASU (1969), 'PM' MARKS THE PIERSON
MOSKOWITZ VALUE

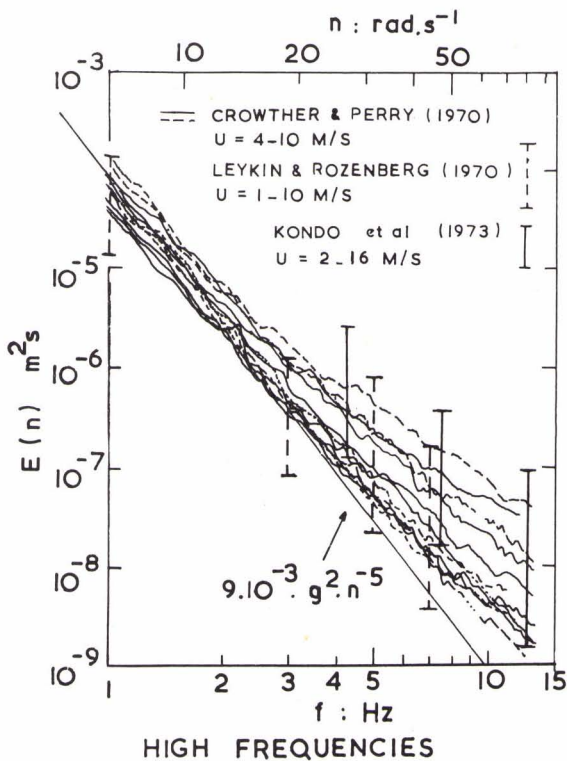
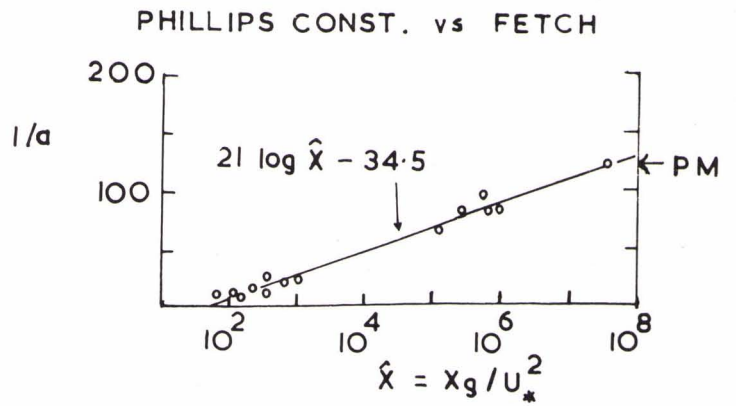
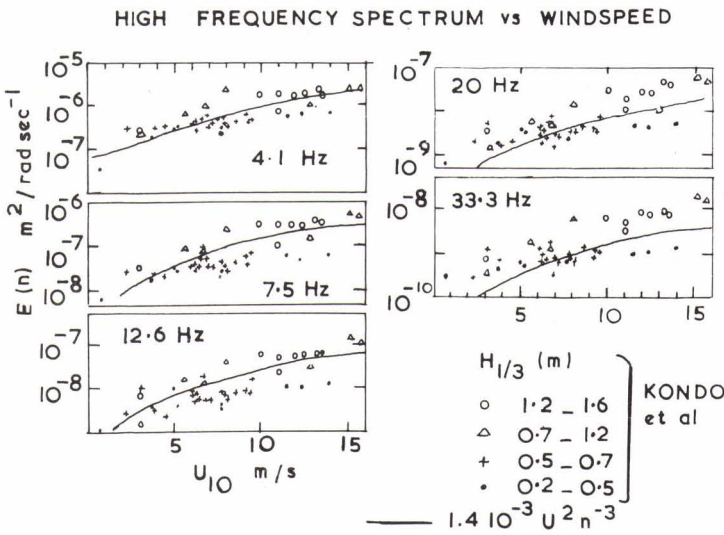


FIG. 7
COLLECTED HIGH FREQUENCY RESULTS, SHOWING
DEPARTURE FROM THE PHILLIPS SPECTRUM

FIG. 8
DEPENDENCE OF HIGH FREQUENCY SPECTRUM ON SEA STATE.
 σ_{pvh}^2 IS SURFACE MEAN SQUARE PARTICLE SPEED,
 U^2 IS WINDSPEED SQUARED, d IS THE COEFFICIENT
 IN $E(n) = d \cdot \sigma_{pvh}^2 n^{-3}$



HIGH FREQUENCY SPECTRA vs SEA STATES

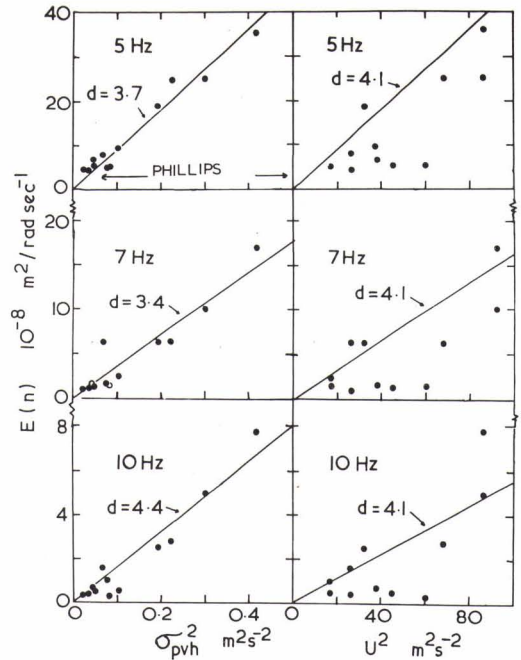


FIG. 9
HIGH FREQUENCY WINDSPEED DEPENDENCE,
 AFTER KONDO ET AL (1973), COMPARED WITH THE
 SPECTRUM AT $d = 4.1$, $E(n) = 1.4 \cdot 10^{-3} U^2 n^{-3}$
 OBTAINED FROM THE DATA OF CROWTHER AND
 PERRY (1970)

PROBE & PHOTO SPECTRA

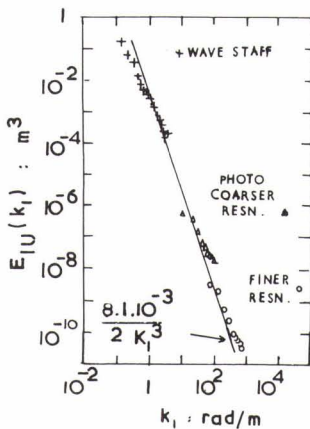


FIG. 10 HIGH FREQUENCY SPECTRA AND
 SIMULTANEOUS PROBE SPECTRA,
 AFTER DOBSON (1970), COMPARED
 WITH THE PIERSON MOSKOWITZ
 SPECTRUM

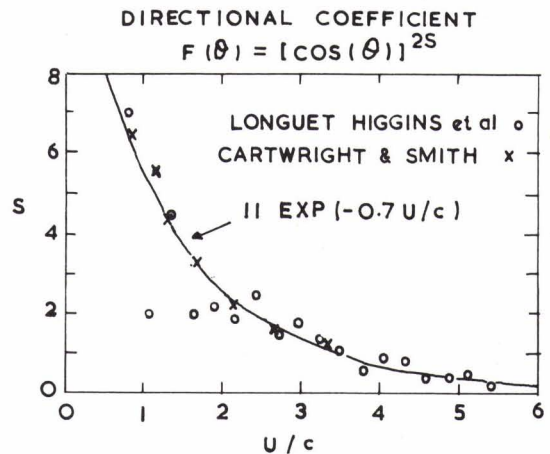


FIG. 11 THE DIRECTIONAL COEFFICIENT VERSUS
 WIND / WAVE SPEED RATIO, USING
 MOTIONAL WAVEBUOYS